Acoustics of Jet Surface Interaction Scrubbing Noise

Abbas Khavaran
Vantage Partners, LLC
NASA Glenn Research Center

20th AIAA/CEAS Aeroacoustics Conference
16 – 20 June 2014, Atlanta GA

Supported by:
NASA Fundamental Aeronautics Program
Fixed Wing Project

Motivation

Interaction of jet exhaust with nearby solid surfaces:

- Hybrid Wing Body (HWB) concepts
- High aspect ratio rectangular exhaust with extended beveled surfaces
- Over the wing engine mount
- Nearby structural components could provide noise shielding
- They could also produce new sources of sound

Measurements*

Rectangular Jet (AR = 8)

M_a = 0.90, h = 0, θ = π/2

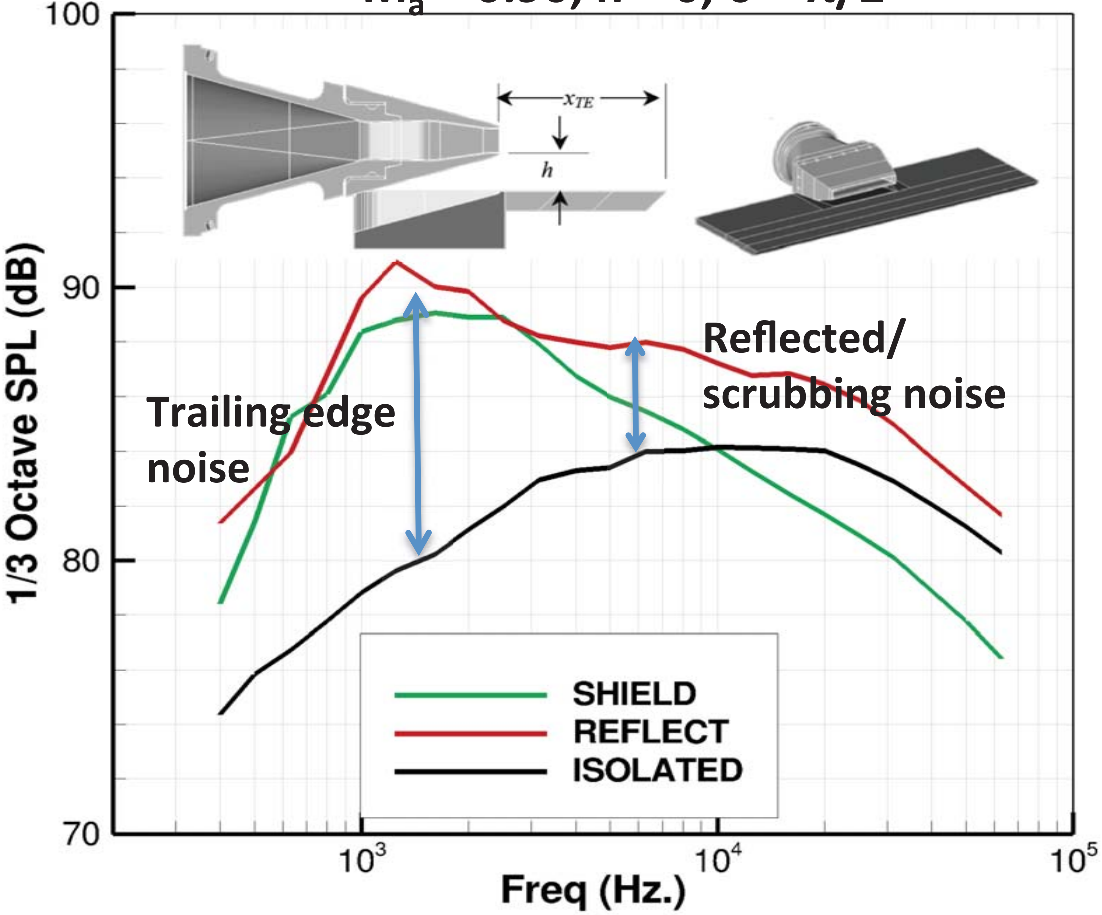

M_a = 0.50, h/D_e =0.45, θ = π/2

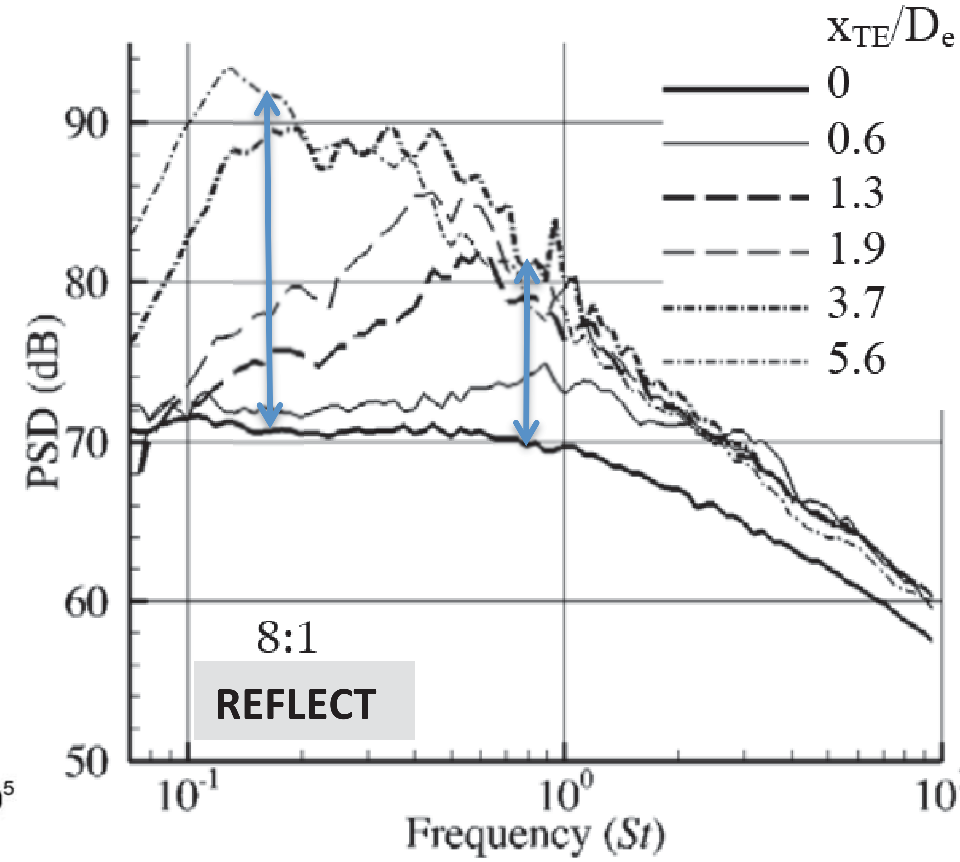

X_{TE} / D_e = 5.6, D_e = 2.14”

* James Bridges, AIAA-2014-0876

Outline

- Governing Equations
- Propagation GF Applicable to High-AR Rectangular Jet
- A Parametric Study of the GF
  - Frequency
  - Temperature
  - Source Location
  - Directivity/ Flight Effect
  - Wall Impedance Effect
  - Reflected / Isolated Jet

Scrubbing Noise

- NS Equations →(Mean Flow + Linear Eqs. for Fluctuations)
- Locally Parallel Mean Flow
- Compressible
- Constant Static Pressure
- Ideal Gas Law

Variable density inhomogeneous PB eq.

$$L\pi' = \Gamma, \qquad \pi' \simeq \frac{p'(\vec{x},t)}{\gamma \bar{p}}$$

$$L \equiv D\left(D^2 - \frac{\partial}{\partial x_j}(c^2 \frac{\partial}{\partial x_j}) \right) + 2c^2 \frac{\partial U}{\partial x_j} \frac{\partial^2}{\partial x_1 \partial x_j}, \quad D \equiv \frac{\partial}{\partial t} + U \frac{\partial}{\partial x_1}$$

- Source term Γ is defined according to the generalized Acoustic Analogy, Goldstein 2010)

Green's Function Method

$$\pi'(\vec{x},t)=\int_{\vec{y}}\int_{\tau} G(\vec{x},t;\vec{y},\tau)\Gamma(\vec{y},\tau)d\tau d\vec{y}$$

$$LG(\vec{x},t;\vec{y},\tau)=\delta(\vec{x}-\vec{y})\delta(t-\tau)$$

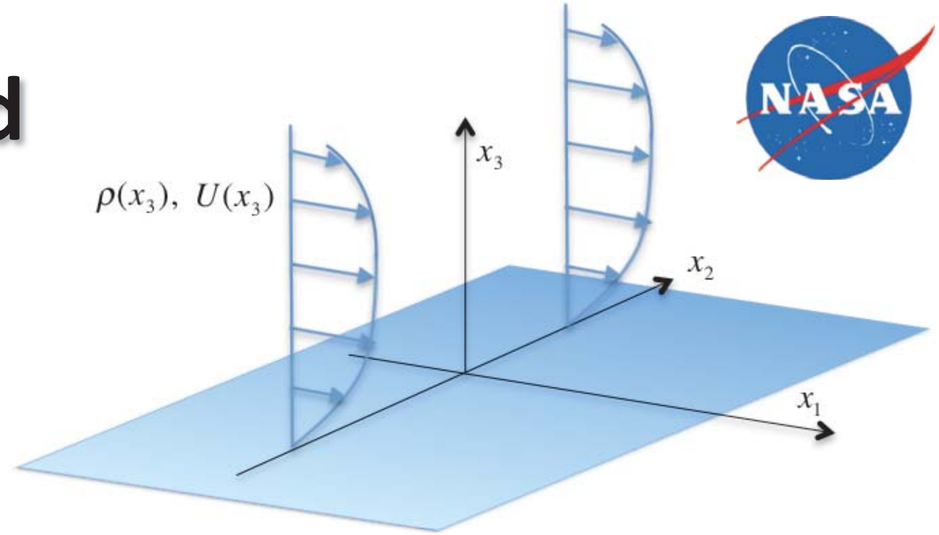

- **Wetted side of the plate only (scattered noise component discussed by Goldstein *et al*, 2013)**

Transform: $(x_1,x_2,t)\rightarrow(k_1,k_2,\omega)$

$$G(\vec{x},t;\vec{y},\tau)\rightarrow\hat{G}(\vec{k}_t,x_3;y_3,\omega) \qquad \vec{k}_t\equiv(k_1,k_2)$$

$$\frac{\partial^2\hat{G}}{\partial x_3^2}+\left(\frac{(c^2)'}{c^2}-\frac{2k_1U'}{-\omega+k_1U}\right)\frac{\partial\hat{G}}{\partial x_3}+\left(\frac{(-\omega+k_1U)^2}{c^2}-k_1^2-k_2^2\right)\hat{G}=\frac{i}{(2\pi)^3}\frac{\delta(x_3-y_3)}{c^2(-\omega+k_1U)}$$

- **Far-field spectral density**

$$\overline{p^2}(\vec{x},\omega)=\int_{\vec{y}}\int_{\vec{\xi}}\int_{\tau=-\infty}^{\infty}\mathbf{G}^*(\vec{x},\vec{y}-\vec{\xi}/2;\omega)\mathbf{G}(\vec{x},\vec{y}+\vec{\xi}/2;\omega)q(\vec{y},\vec{\xi},\tau)e^{i\omega\tau}d\tau d\vec{\xi}d\vec{y}$$

GF Method (cont'd)

- The Eq is re-arranged into a self-adjoint 2nd order ODE
- Two linearly independent solutions $V_j(\vec{k}_t, x_3, \omega),\ j = 1,2$

$$V_j'' + f(\vec{k}_t, x_3, \omega) V_j = 0$$

IVP

$$x_3 = 0 \quad \left| \begin{array}{l} V_1(x_3) = 1 \\ \dfrac{\partial V_1(x_3)}{\partial x_3} - \psi V_1(x_3) = 0, \end{array} \right. \qquad \psi(k_1, \omega, \bar{Z}) = \left(\frac{i\kappa_o}{\bar{Z}} \frac{c_\infty^2}{c^2(0)} + \frac{c'(0)}{c(0)} + \frac{k_1}{\omega} U'(0) \right)$$

$$\bar{Z}(\omega) = \frac{(\hat{p}' / \hat{v}_3')}{\rho_\infty c_\infty}$$

BVP

$$\left| \begin{array}{l} V_2(x_3) = 1, \quad x_3 = 0 \\ \dfrac{\partial V_2(x_3)}{\partial x_3} + i\chi_\infty V_2 = 0, \quad x_3 \to \infty \end{array} \right.$$

- Radiation condition

$$\chi_\infty^2 \equiv (-\kappa_o + k_1 M_\infty)^2 - k_1^2 - k_2^2 > 0, \quad \kappa_o = \omega / c_o$$

GF Method (cont'd)

$$\mathbf{G}(\vec{x},\vec{y};\omega)=\frac{i}{(2\pi)^3}\frac{1}{c(y_3)c(x_3)}\int_{k_1}\int_{k_2}\frac{-\omega+k_1U(x_3)}{\left(-\omega+k_1U(y_3)\right)^2}\frac{b_2V_1(\vec{k}_t,y_3,\omega)}{W_o(\vec{k}_t,\omega,\bar{Z})}e^{i\Theta(\vec{k}_t,\vec{x},\omega)}dk_1dk_2$$

$$\Theta(\vec{k}_t,\vec{x},\omega)=k_1(x_1-y_1)+k_2(x_2-y_2)-\chi_\infty x_3$$

$$V_2(\vec{k}_t,x_3,\omega)=b_2(\vec{k}_t,\omega)e^{-i\chi_\infty x_3} \qquad x_3\to\infty$$

- Stationary Phase solution $(\kappa_o R \gg 1,\ \kappa_o=\omega/c_\infty)$

$$\vec{k}_t^{\,s}=\kappa_o(\sin\phi^s\cos\theta^s,\ \cos\phi^s)$$

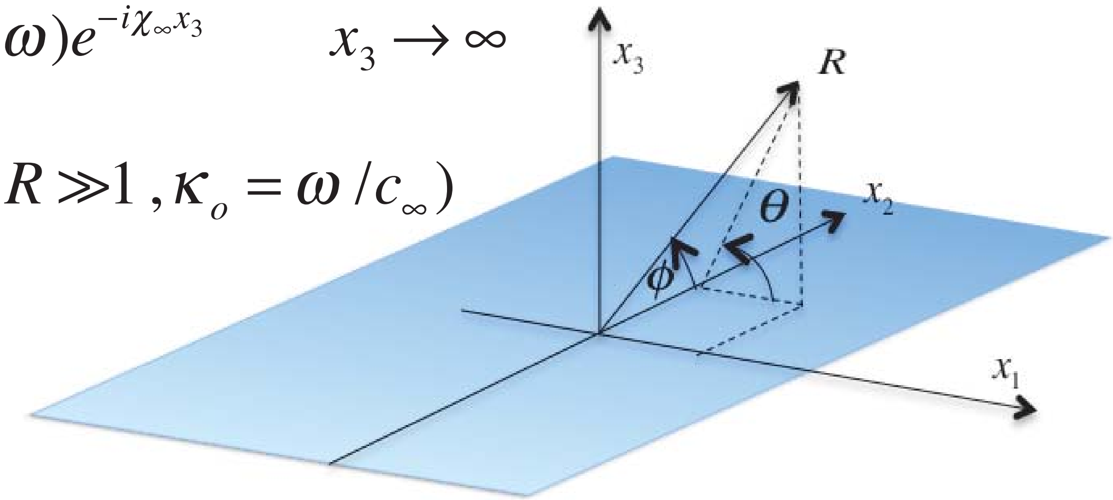

$$0\le\theta\le\pi,\ 0\le\phi\le\pi$$

$$\mathbf{G}(\vec{x},\vec{y};\omega)\sim -i\frac{e^{i\Theta(\vec{k}_t^{\,s},\vec{x},\omega)}}{(2\pi)^3R}\frac{\sin\theta^s\sin^2\phi^s}{c_\infty^2c(y_3)}\frac{b_2(\vec{k}_t^{\,s},\omega)V_1(\vec{k}_t^{\,s},y_3,\omega)}{W_o\left(\vec{k}_t^{\,s},\omega,\bar{Z}\right)}\frac{\Im}{\left(1-\frac{U(y_3)}{c_\infty}\sin\phi^s\cos\theta^s\right)^2}$$

Stationary-Phase Point

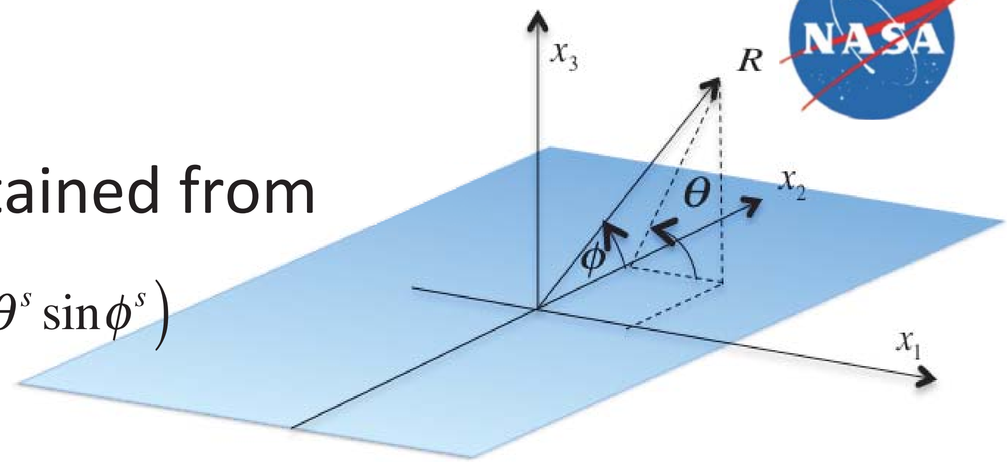

- Stationary point angles are obtained from

$$\tan\theta = -S(\theta^s,\phi^s,M_\infty)/\left(M_\infty + (1-M_\infty^2)\cos\theta^s \sin\phi^s\right)$$

$$\sin\theta \tan\phi = -S(\theta^s,\phi^s,M_\infty)/\cos\phi^s$$

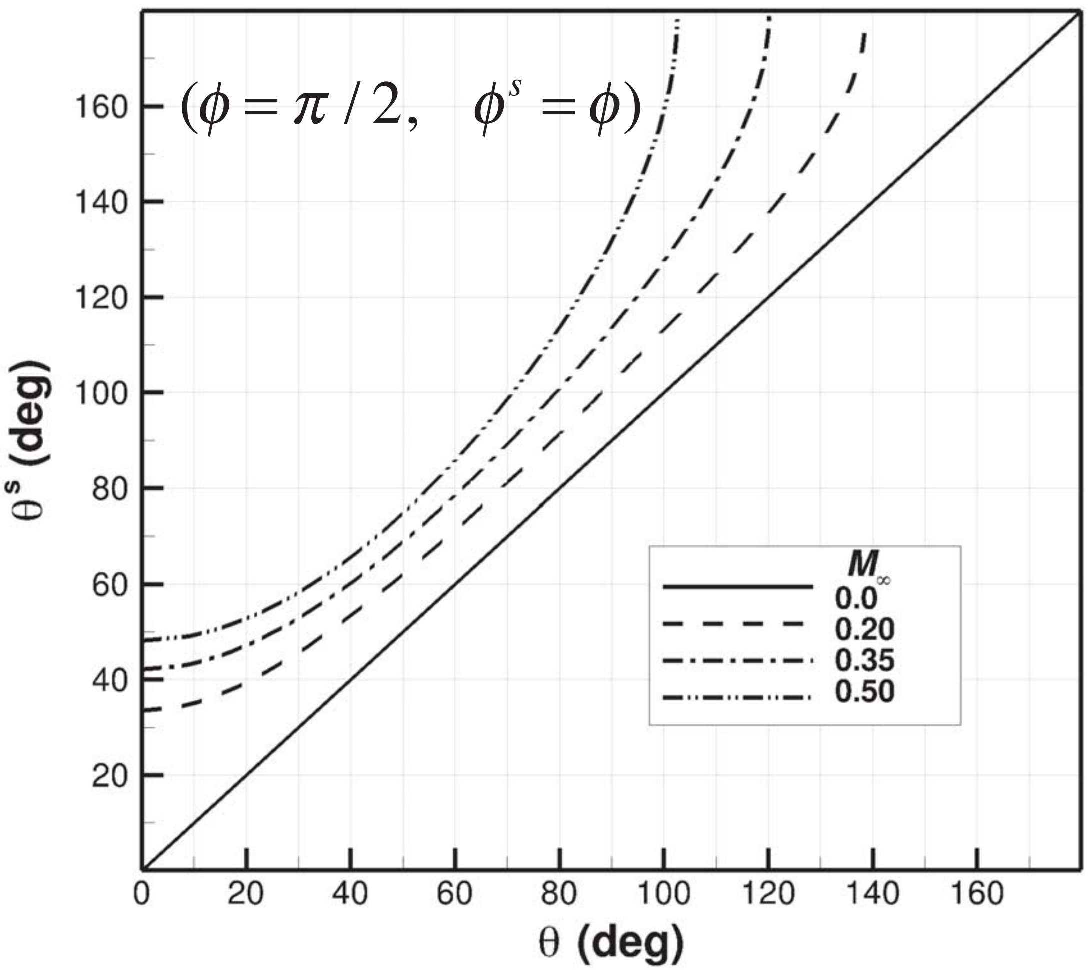

Temperature & Velocity Profiles

$$(M_\infty = 0, U_j / c_\infty = 0.90)$$

- **Analytical profiles are selected for mean velocity & static temperature**

$$\eta = y_3 / D_j$$

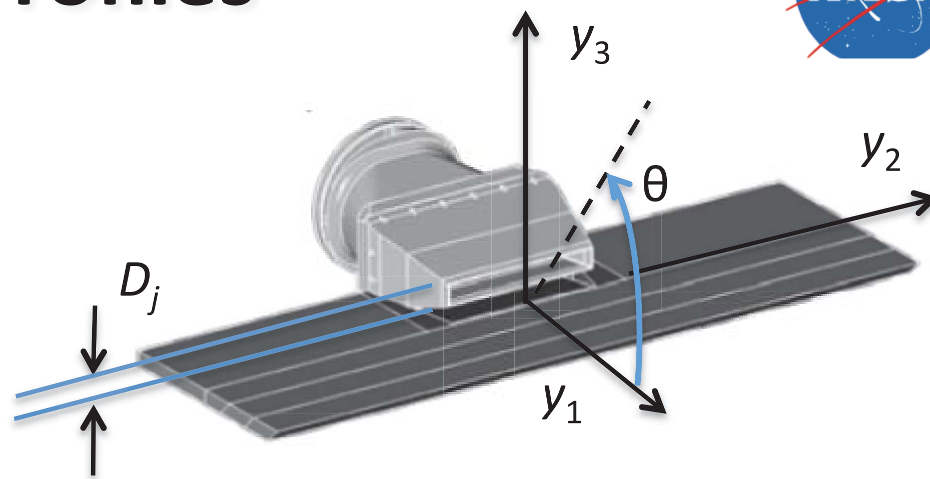

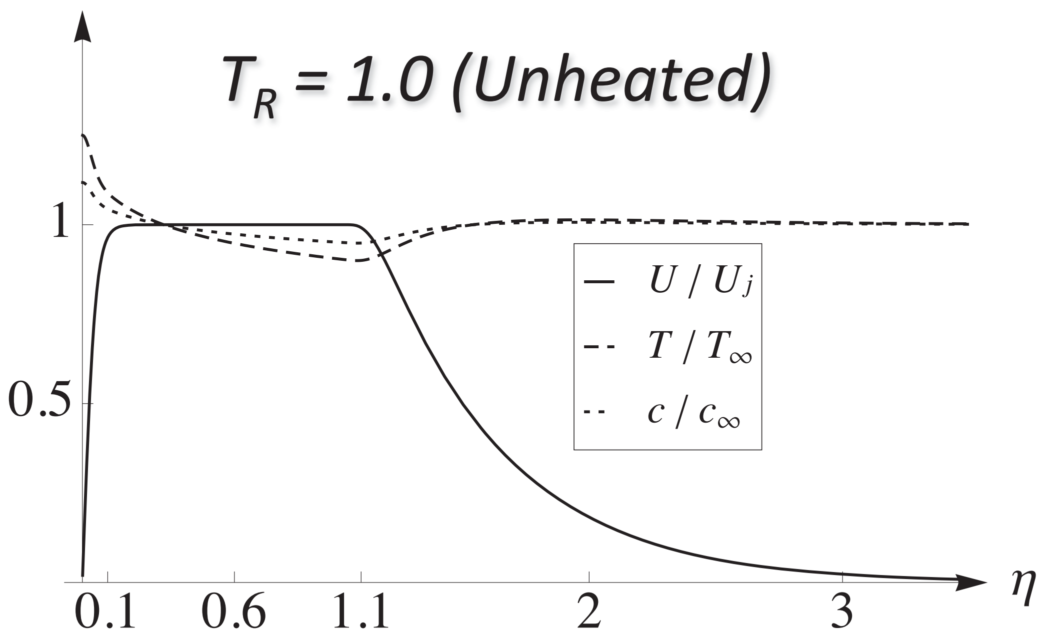

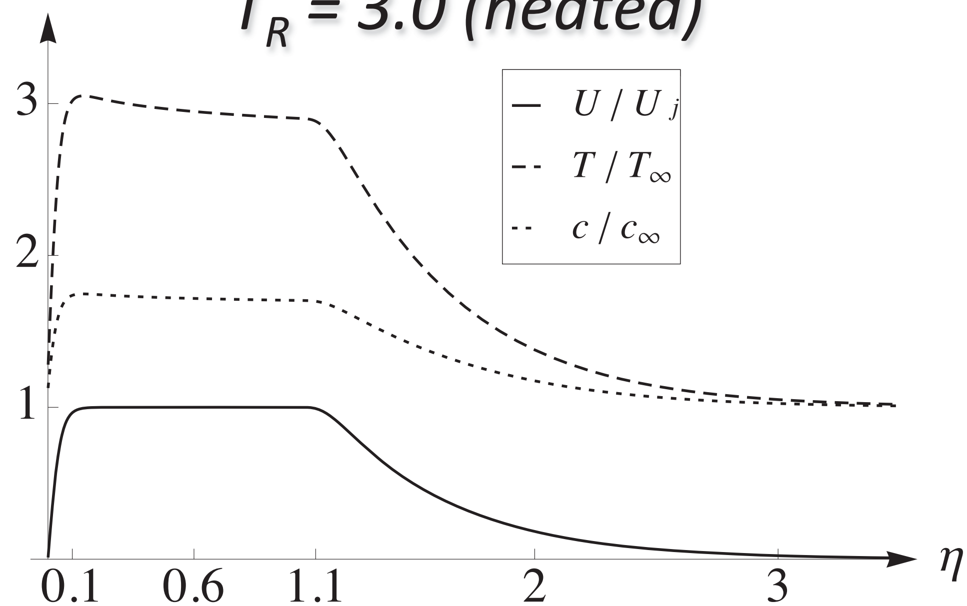

Numerical Results

$(\phi = \pi/2, \theta = \pi/4, U_j/c_\infty = 0.90, T_R = 3.0)$

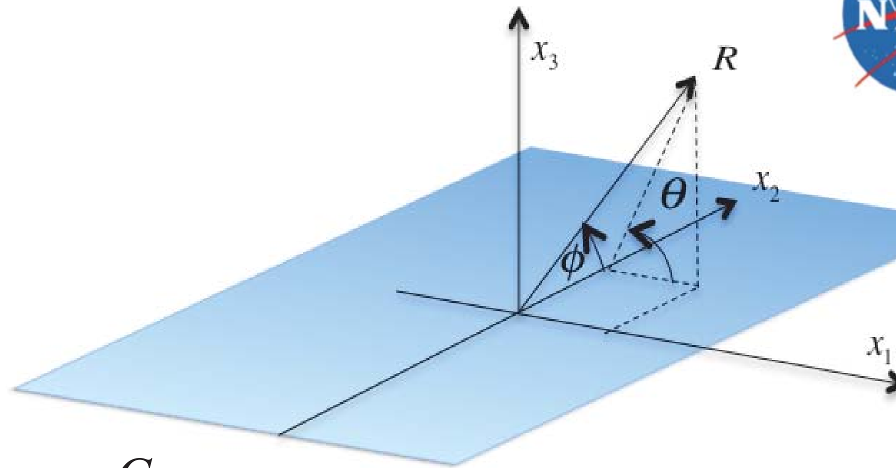

- Normalized GF $G_N \equiv \dfrac{\pi c_\infty^3 \mathbf{G}}{G_{FS}}$

$$St \equiv \frac{\omega D_j}{2\pi U_j}$$

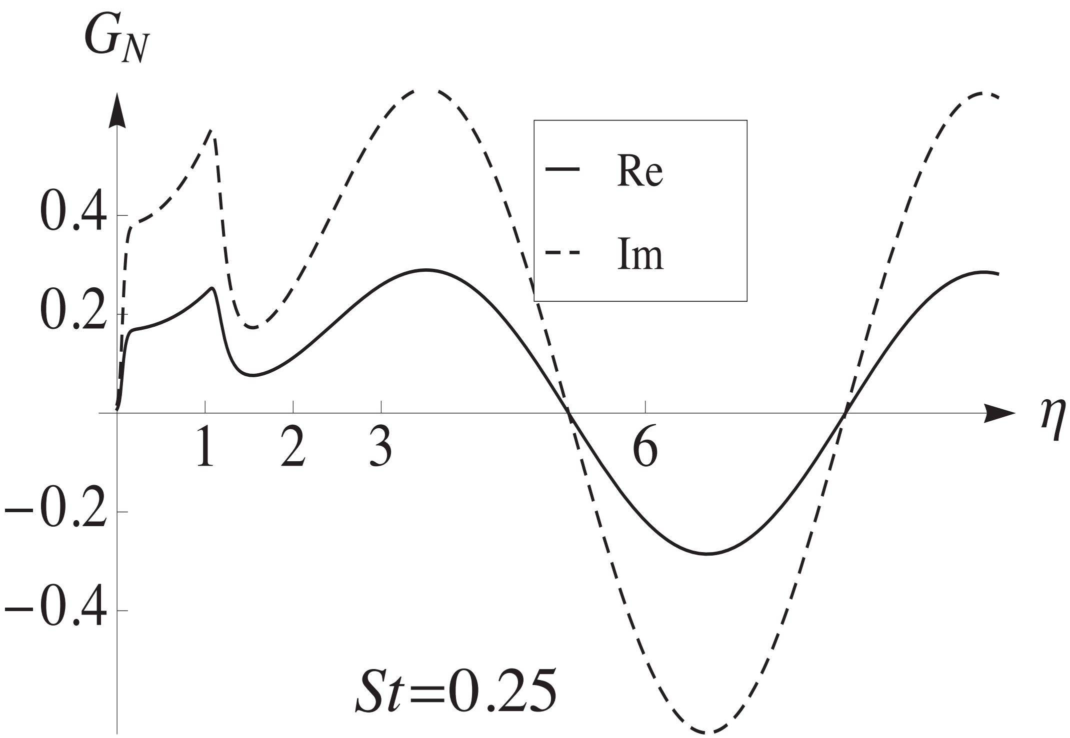

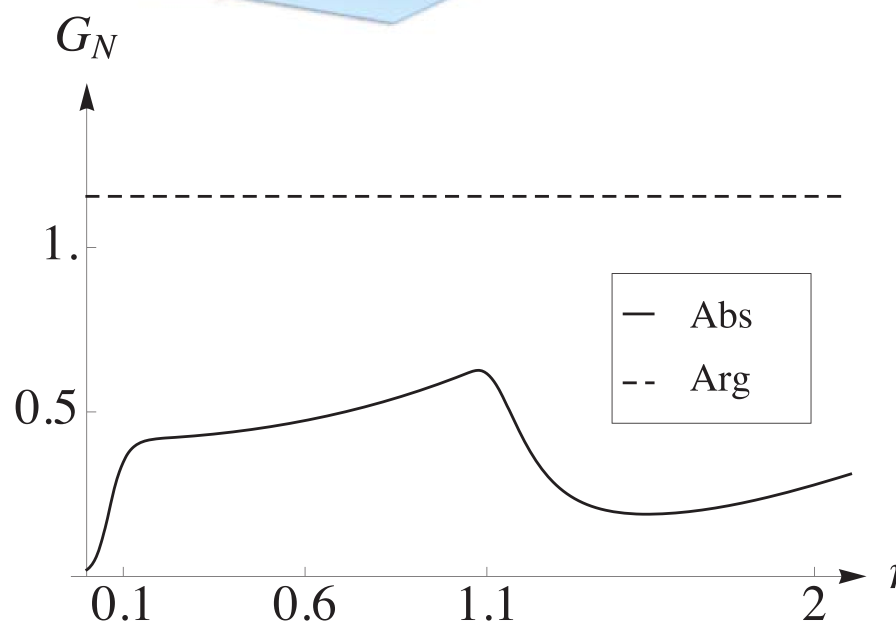

Effect of Frequency

$(\phi = \pi/2, \theta = \pi/4, U_j/c_\infty = 0.90, T_R = 3.0)$

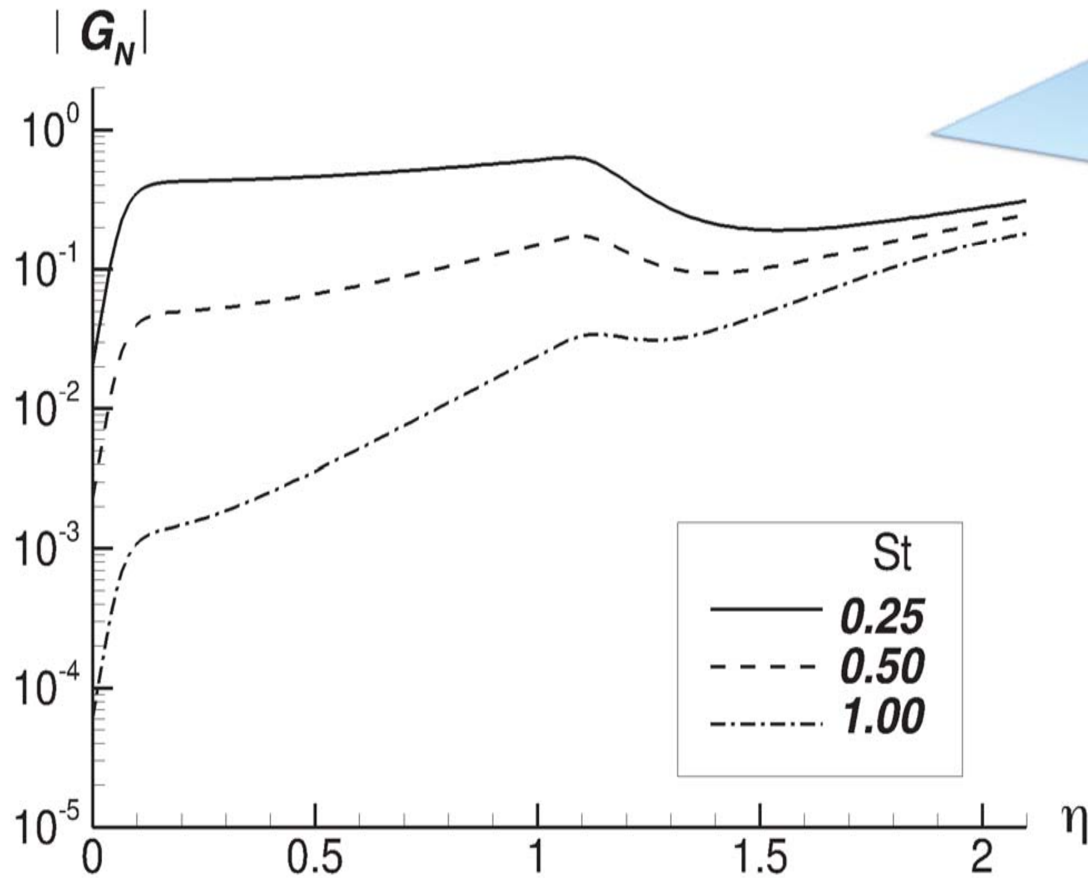

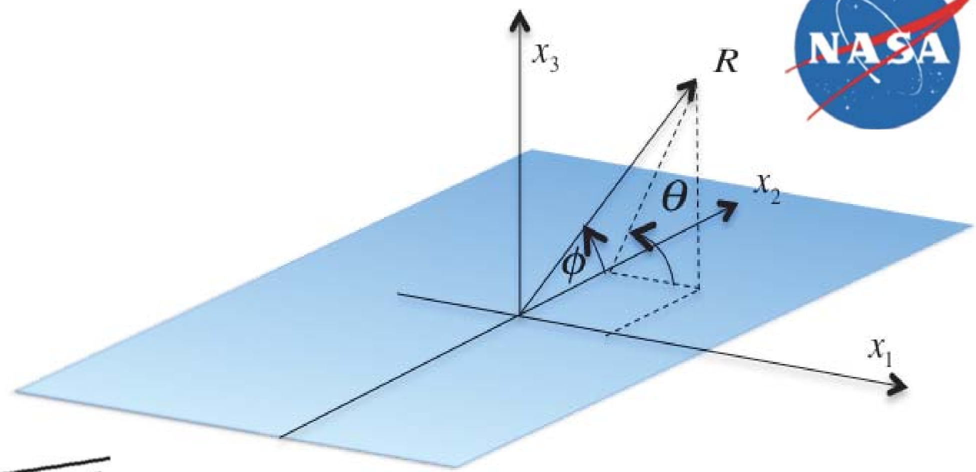

$$St \equiv \frac{\omega D_j}{2\pi U_j}$$

- **GF amplitude decreases with increasing frequency**
- **In a uniform mean flow $G_N \sim 1/\omega$**

Effect of Temperature

$(\phi = \pi/2, \theta = \pi/4, St_o = 0.25, U_j/c_\infty = 0.90)$

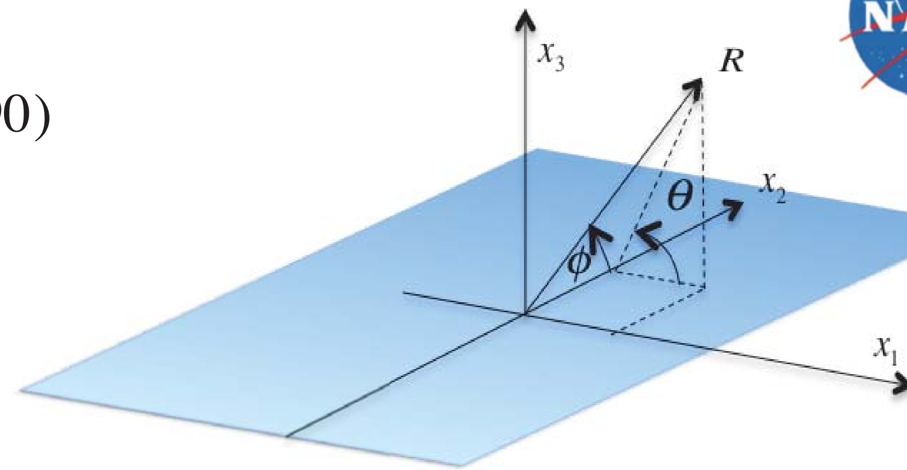

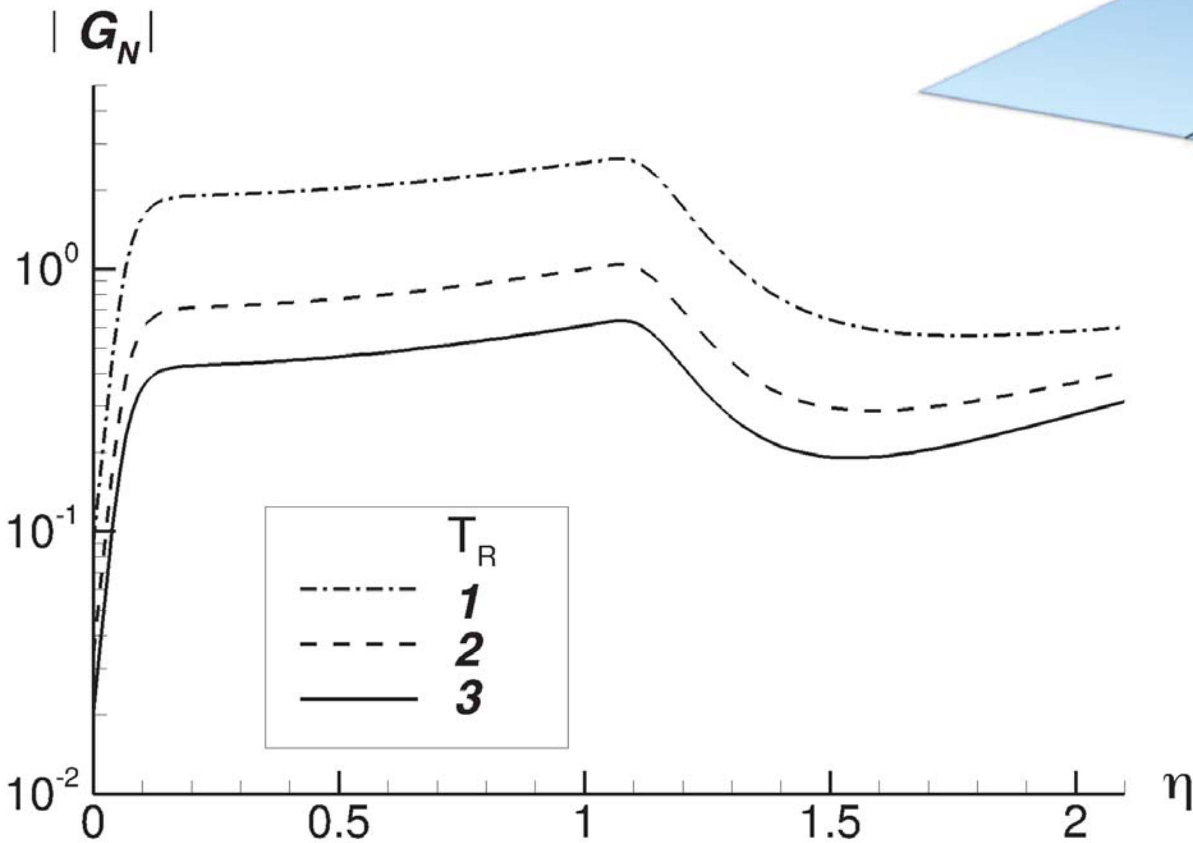

- **GF amplitude decreases with increasing temperature**

Effect of Surface Impedance

$(\phi = \pi/2, \theta = \pi/4, St_o = 0.25, U_j/c_\infty = 0.90, T_R = 1.0)$

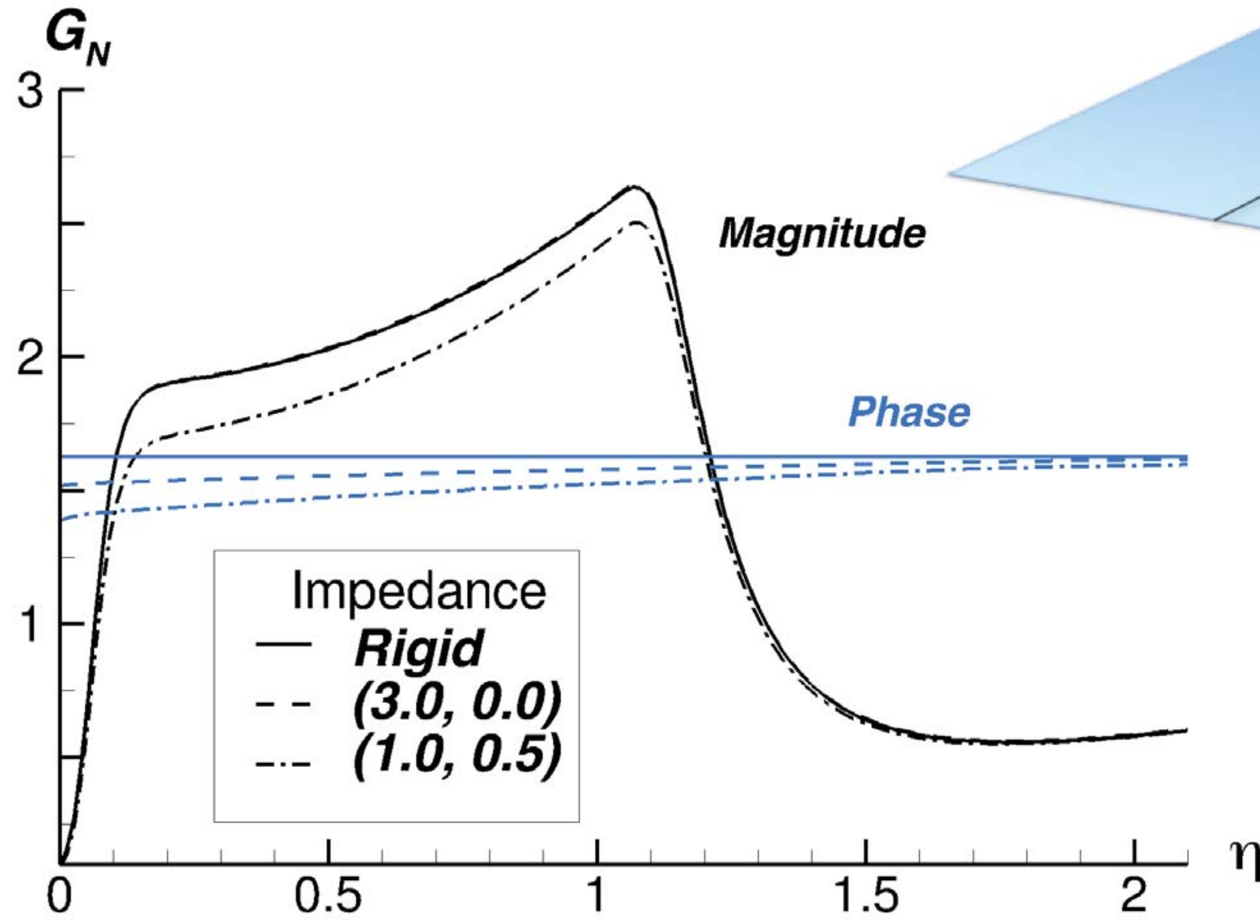

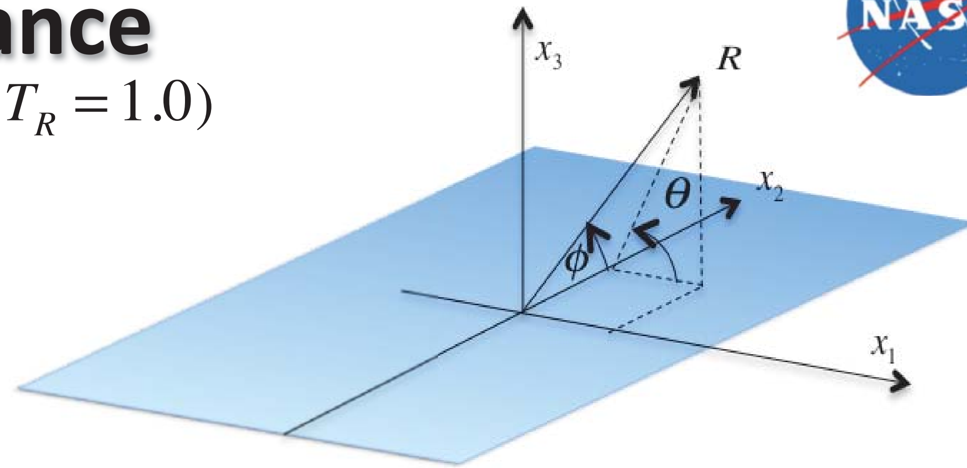

- Phase factor depends on source location for non-rigid surface

Flight Effect on Directivity

$(\phi = \pi/2, St_o = 0.25, U_j/c_\infty = 0.90, T_R = 1.0)$

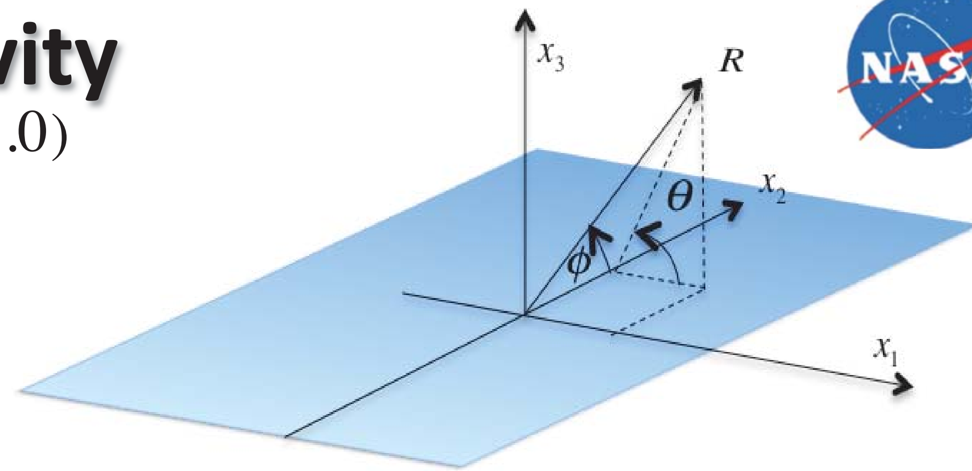

M$_\infty$=0.0

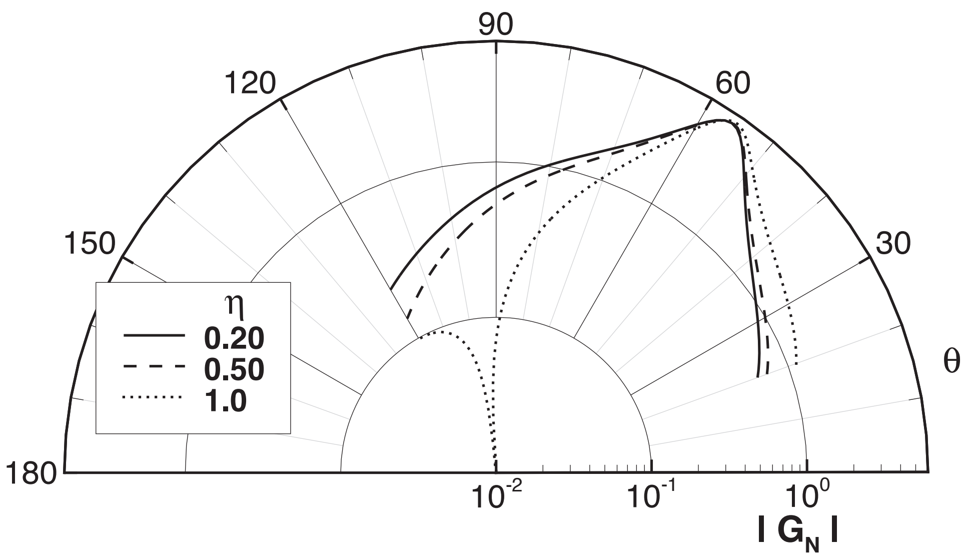

St = 0.25, Uj = 0.90, TR = 10, Ma = 0.0, Z = Rigid, $\phi=\pi/2$

M$_\infty$=0.35

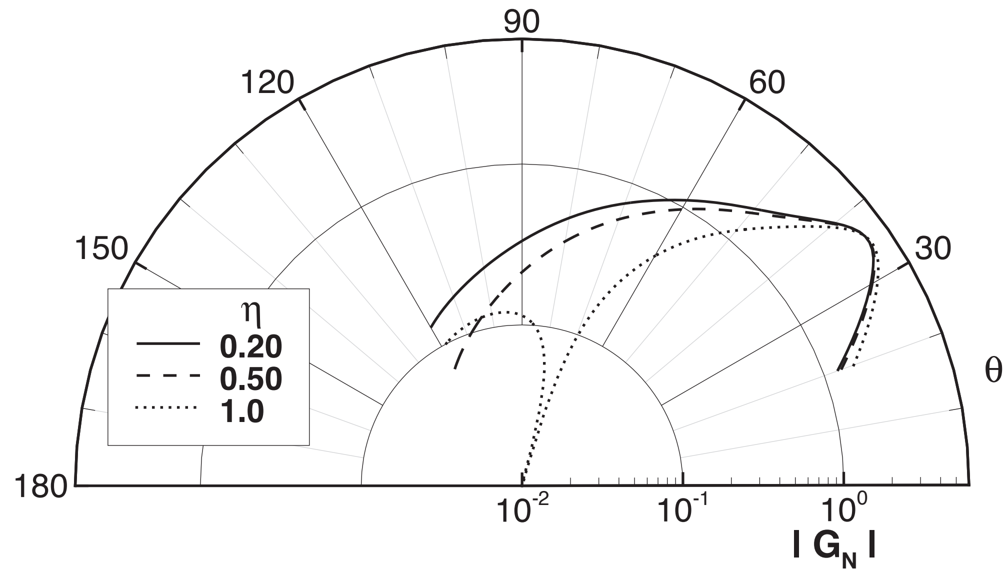

St = 0.25, Uj = 0.90, TR = 1.0, Ma = 0.35, Z = Rigid, $\phi=\pi/2$

- **GF peaks at smaller down-stream angles as flight Mach number is increased**

Isolated Rectangular Jet

$$V_j(x_3) = 1, \quad x_3 \to -\infty, \quad j = 1,2$$

$$\frac{\partial V_j}{\partial x_3} - (-1)^j \, i\chi_\infty V_j = 0, \quad x_3 \to \begin{vmatrix} -\infty, & j = 1 \\ +\infty, & j = 2 \end{vmatrix}$$

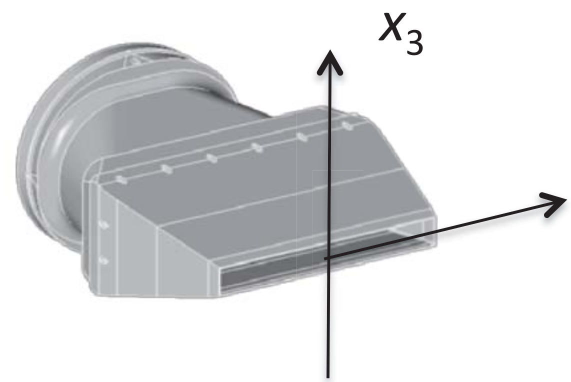

Jet Profile – Unheated

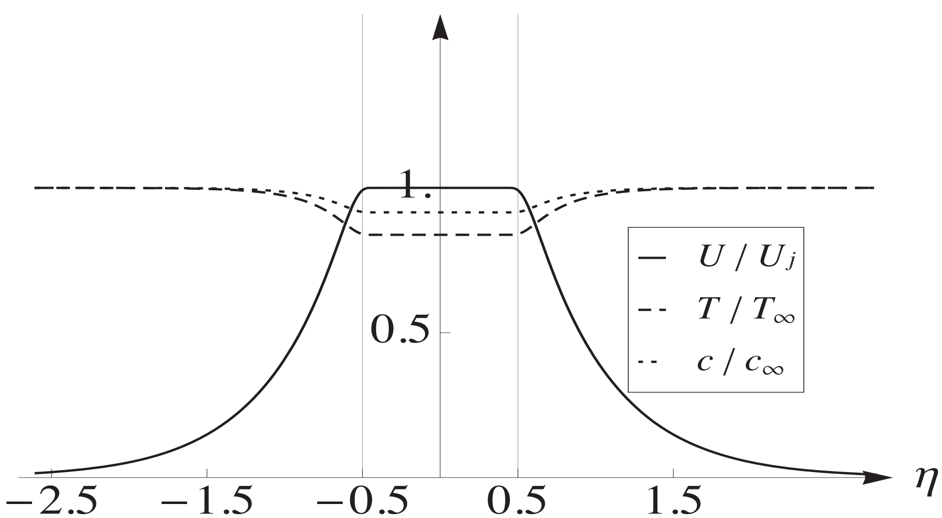

$$\eta = y_3 / D_j$$

Observer at $x_3 \to +\infty$

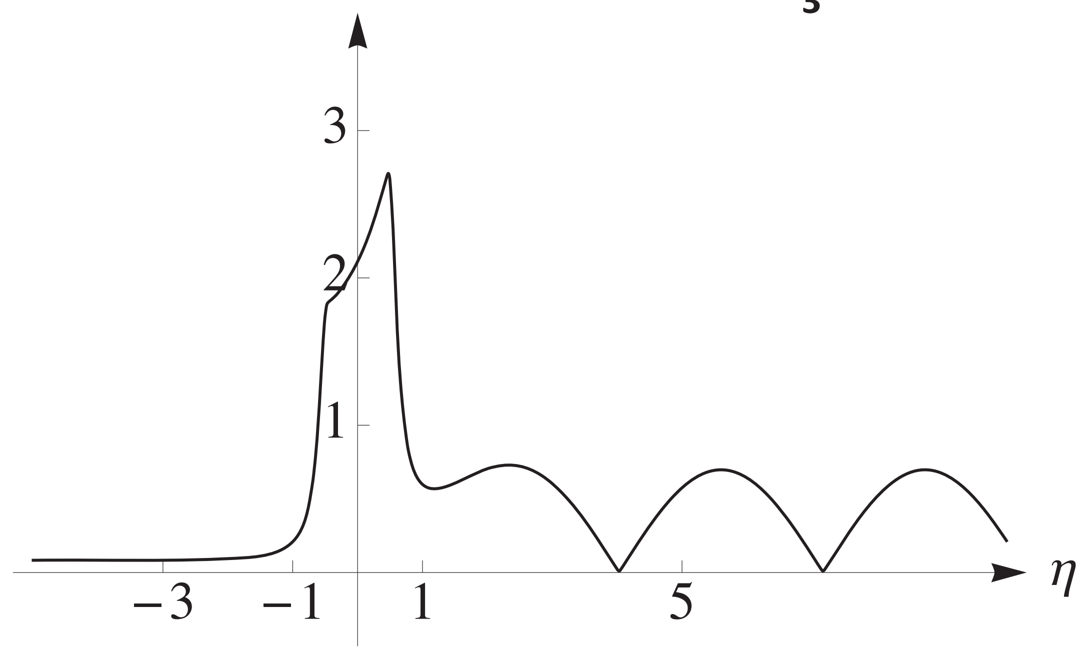

$$(\theta = \pi / 4, St_o = 0.25, U_j / c_\infty = 0.90, T_R = 1.0)$$

Isolated vs. Reflected Jet

(M_a=0.90, T_R=1.0)

GF Directivity (St = 0.25)

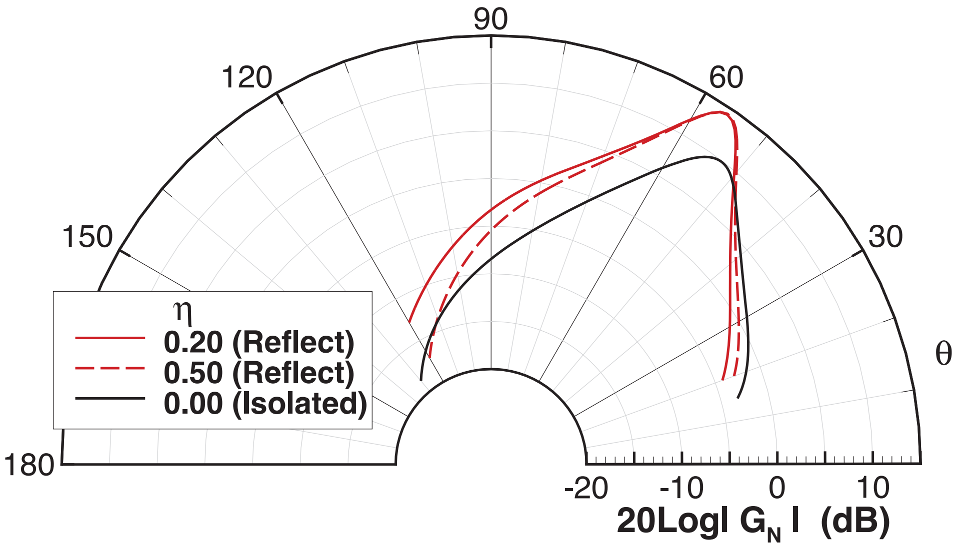

St_b = 0.25, Uj = 0.90, TR = 1.0, Ma = 0.0, $\phi=\pi/2$

Measured SPL (St = 0.28, AR=8)

James Bridges, 2014

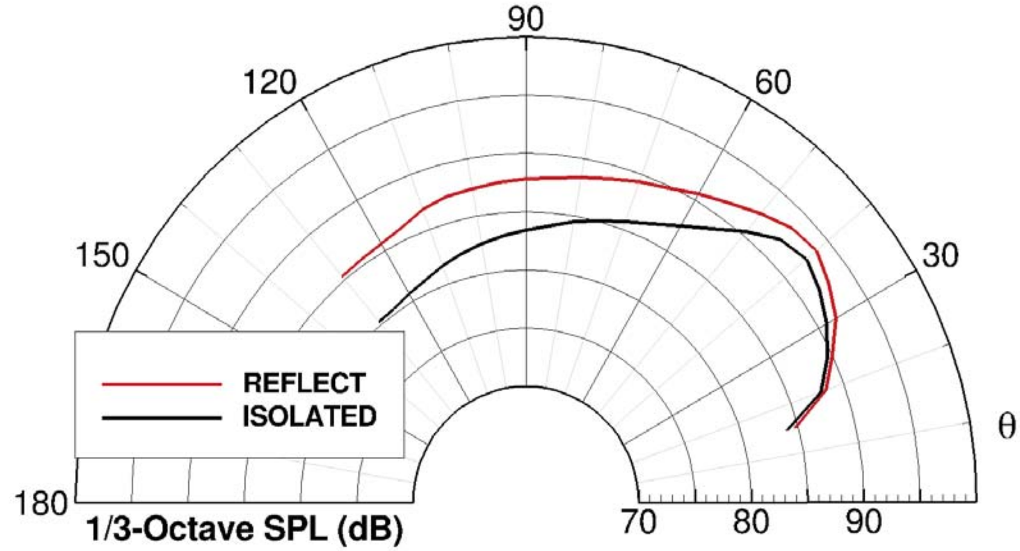

$X_{TE} / D_e = 5.6$, $D_e = 2.14''$

- **A reflecting surface enhances the GF (5-6 dB) relative to an isolated jet (at polar angles larger than peak directivity angle)**

Summary

Within the region of nonzero sources:

- GF magnitude decreases with increasing frequency
- GF magnitude decreases with increasing temperature
- At a fixed polar angle GF magnitude varies with source location, generally increases at smaller downstream angle
- Phase factor varies with source location for non-rigid surface impedance
- GF peaks at smaller down-stream angles as flight Mach number is increased
- Presence of a reflecting surface enhances the GF magnitude (5-6 dB) relative to an isolated jet at polar angles larger than peak directivity angle.

QUESTIONS ?

Measurements (JSIT Tests*)

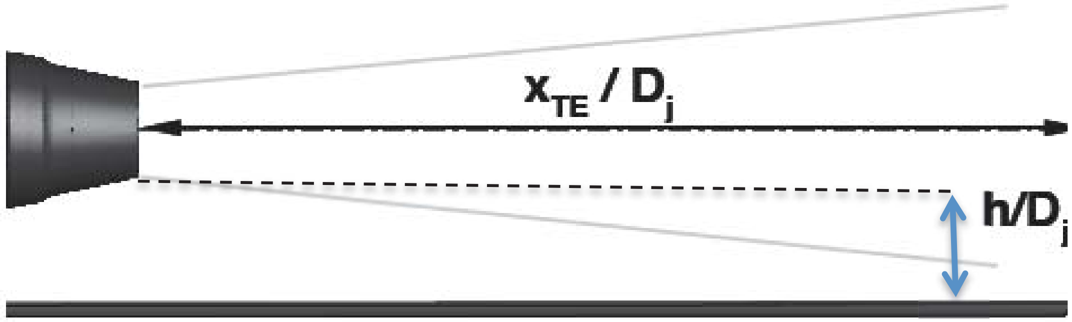

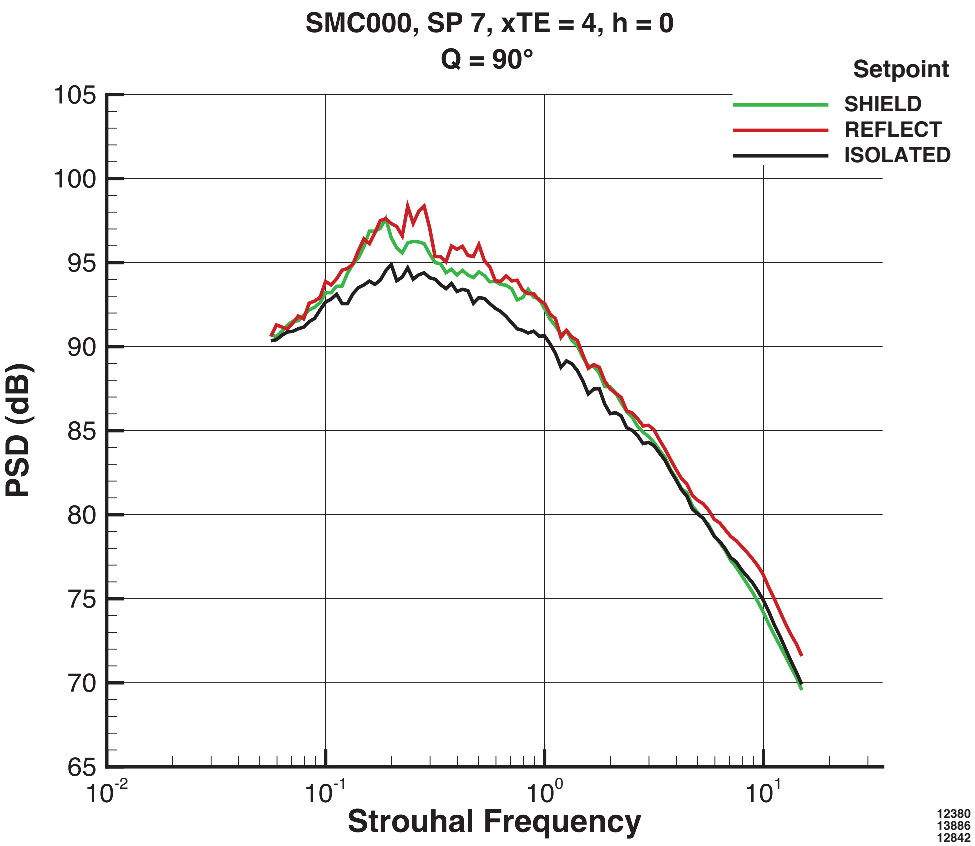

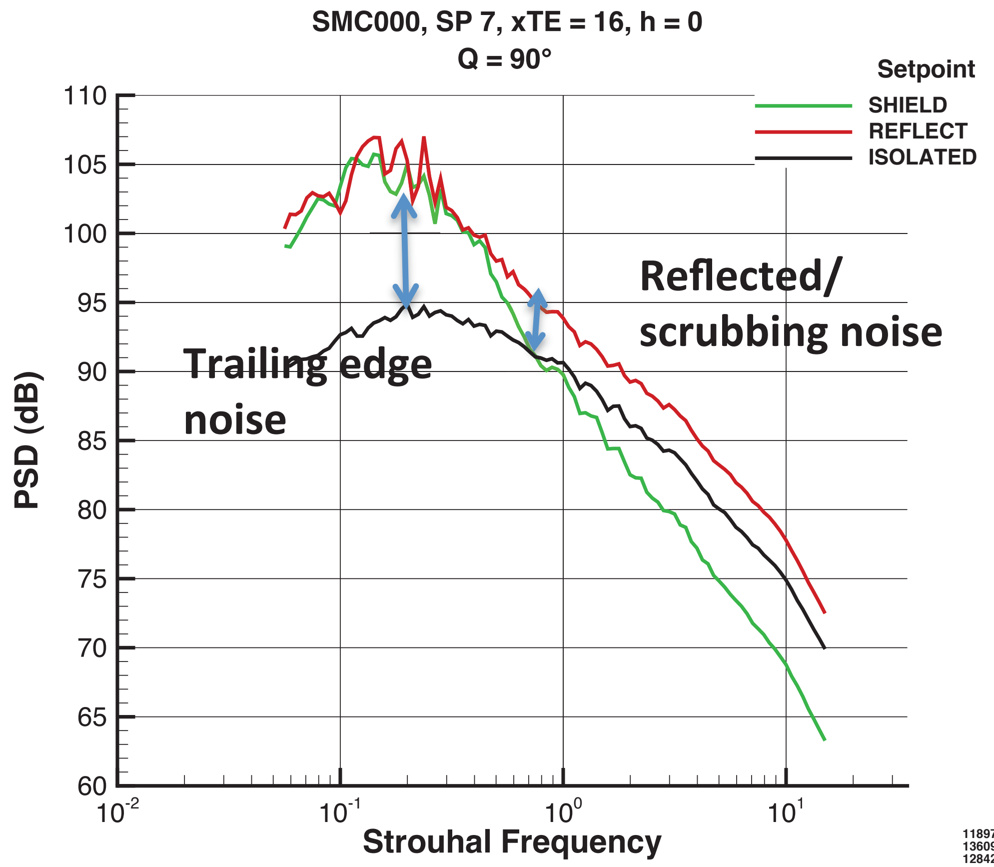

*Cliff Brown (GRC), ASME paper GT2012

*Gary Podboy (GRC), ASME paper GT2012

Mean Flow – Analytical Profiles

- Axial Velocity $\eta = y_3 / D_j$

$$\frac{U(\eta)}{U_j} = \begin{cases} \tanh(\dfrac{D_j \eta}{d_1}), & \eta < 1.05 \\ \dfrac{1}{2}(1+\dfrac{U_\infty}{U_j}) + \dfrac{1}{2}(1-\dfrac{U_\infty}{U_j}) \tanh \dfrac{1}{d_2}\left(\dfrac{1/2}{\eta - 1} - \dfrac{\eta - 1}{1/2} \right), & \eta \geq 1.05 \end{cases}$$

- Temperature

$$T = T_1 + T_2$$

$$\frac{T_1(y_3)}{T_\infty} = 1 + (T_R - 1)\frac{U(y_3)}{U_j} - \frac{\gamma - 1}{2}\left(\frac{U(y_3)}{c_\infty} \right)^2$$

Crocco-Busemann Law

$$\frac{T_2(y_3)}{T_\infty} = \frac{1}{d_3}\left(\frac{1}{2} + \frac{1}{2}\tanh \frac{1}{d_4}(\frac{1}{D_j \eta} - D_j \eta) \right)$$

Frictional heat near the wall

$D_j = 2"$ $\delta_o / D_j = 1.32 d_1$ $(d_1, d_2, d_3, d_4) = (0.10, 2, 4, 3)$

Effect of Observer Angle

$(\phi = \pi/2, St_o = 0.25, U_j/c_\infty = 0.90, T_R = 3.0)$

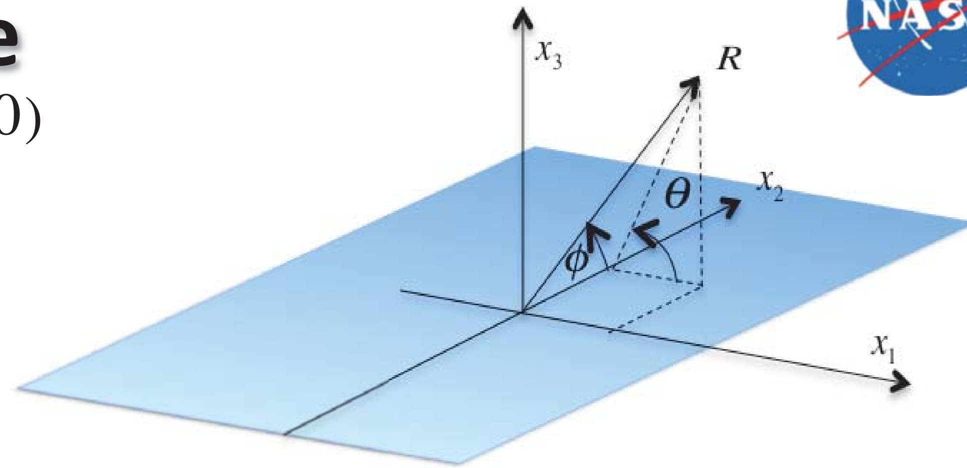

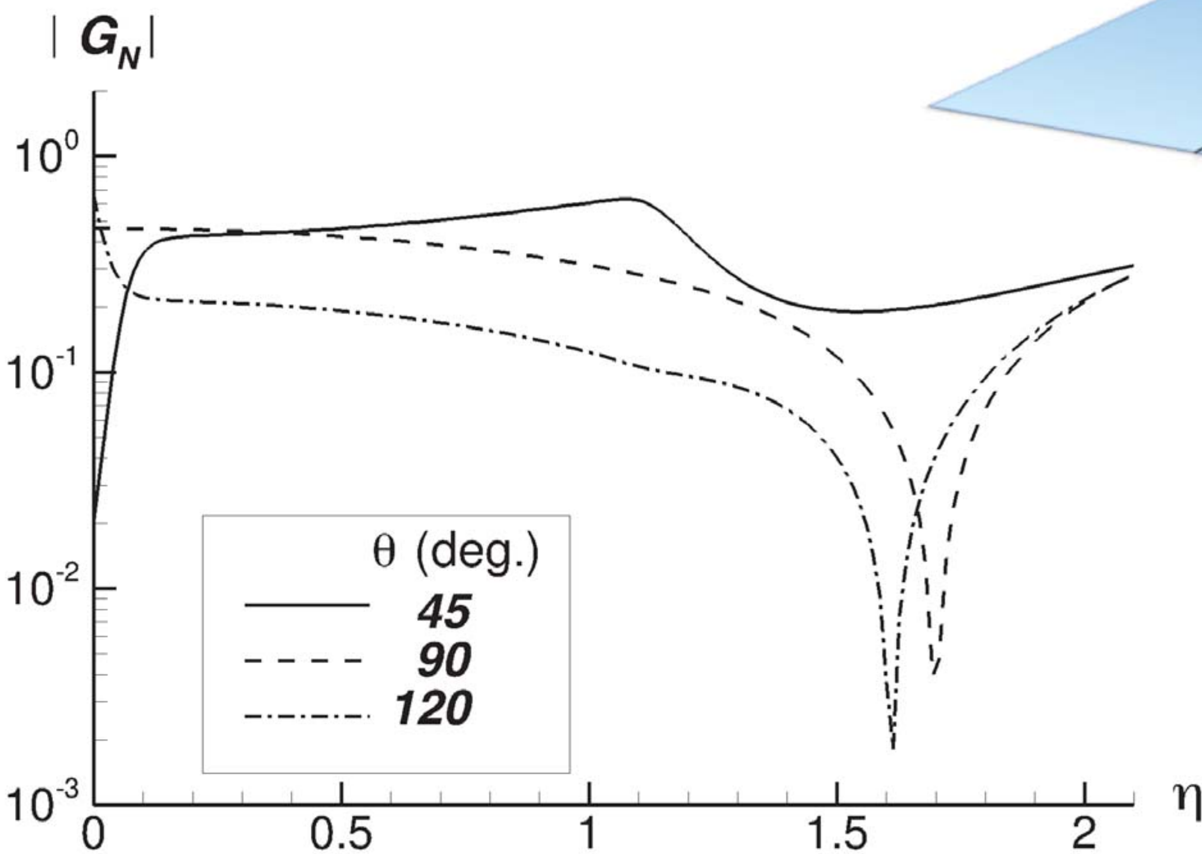

- **GF amplitude varies with source location, generally increases at smaller downstream angles**